lubricants

MDPI

Article

Enhancing the Lubrication Performance of Steel–Steel Contacts Using a Novel Ionic Liquid Based on Phosphate Ammonium Salt as an Oil Additive

Junjie Xie [1], Shuai Hu [2,3], Cunqiang Liu [1], Ziqiang Gao [1], Faxue Zhang [1], Chaoyang Zhang [2,3,*] and Mohamed Kamal Ahmed Ali [3,4,*]

[1] Gansu Road & Bridge Construction Group Co., Ltd., Lanzhou 730030, China
[2] Shandong Laboratory of Yantai Advanced Materials and Green Manufacturing, Yantai 264000, China
[3] State Key Laboratory of Solid Lubrication, Lanzhou Institute of Chemical Physics, Chinese Academy of Sciences, Lanzhou 730000, China
[4] Automotive and Tractors Engineering Department, Faculty of Engineering, Minia University, El-Minia 61519, Egypt
* Correspondence: 13259863531@163.com (C.Z.); eng.m.kamal@mu.edu.eg (M.K.A.A.)

Abstract

Oil additives are essential for improving anti-wear (AW) properties and durability of mechanical components. In this study, a novel ionic liquid based on phosphate ammonium salt (coded as IL-NPAS) was designed using organic synthesis methods. The high-level objective of this work is to enhance the wear resistance ability of oil-lubricated steels with low-cost additives in terms of materials and manufacturing methods. The IL-NPAS additive was incorporated at concentrations of 0.1 wt% and 0.5 wt% in 150 SN oil, which served as the base oil. Additionally, the commercial oil additive (coded as AW6110) was utilized as a reference to evaluate the effectiveness of the synthesized additive. The frictional behaviour was evaluated with an SRV tribometer at test temperatures of 25 °C and 100 °C. After that, SEM, 3D profilometry, XPS, and TOF-SIMS techniques were employed to show the wear modes and determine the chemical composition of the lubricating tribolayer. Noticeably, the formulated lubricant based on the 0.5 wt% IL-NPAS additive provided AW performance almost identical to the AW6110 additive. The results showed that the 0.5 wt% IL-NPAS additive reduced the coefficient of friction (COF) and improved AW properties by 34–36% and 80–90%, respectively, compared to the 150 SN base oil. Overall, this study holds significant promise for the development of low-cost lubricating oil additives.

Keywords: oil additives; ionic liquids; friction; wear; lubrication mechanism

Received: 1 December 2025
Revised: 27 December 2025
Accepted: 30 December 2025
Published: 4 January 2026

1. Introduction

Effective oil additives play a vital role in energy saving, minimization of material wear, and extension of the service life of mechanical tribosystems [1–3]. Hence, superior lubrication performance is contributing significantly to sustainability and cost-effectiveness in industrial operations. Lubricant additives play a vital role in novel lubricating oils that are designed for superior performance [4,5]. These additives significantly improve the thermo-physical-chemical properties of lube oils, either by introducing novel features or by enhancing their current performance to meet stringent tribological and environmental requirements [6,7]. The comprehensive effectiveness of lubricating oil is largely dependent on the development of oil additive technology [8]. Therefore, the technological progress,

industrial scaling, and practical application of novel oil additives substantially influence the development of tribological systems for saving energy [9]. In this context, researchers and tribologists have focused on synthesizing new oil additives to improve the lubrication performance of tribosystems [10,11]. Phosphorus-based additives have been a staple in lubricating oils and greases for decades, mainly comprising phosphate and hypophosphite compounds [12–14]. Among these, phosphate esters have gained prominence, with triphenyl phosphate ester (TCP) standing out as the most prestigious [15]. The utilization of TCP as a severe pressure anti-wear addition may be traced back to the 1940s and 1950s, with a research history that spans over 80 years [16]. TCP is utilized as an oil addition in a wide range of lubricant formulations, such as cutting oils, gear lube oils, lubricating greases, and drilling fluids [17,18]. Additionally, the continued use of ionic liquids based on phosphorus additives confirms their importance in improving tribological performance for e-mobility applications [19].

Regarding AW mechanisms of phosphate esters, some studies showed that phosphate esters decompose under high-temperature conditions on the friction surfaces [20]. After that, the decomposition products undergo a reaction with iron that is already on the contact surface, promoting the formation of iron phosphide to create a low-melting-point eutectic layer [21,22]. This layer significantly enhances the surface smoothness of the metal substrate by filling in surface imperfections and concave flaws. This is known as the "chemical polishing effect," which improves AW properties. Additionally, the smoother surface contributes significantly to the reduction in boundary friction [23]. According to the literature [24], some studies demonstrated that the formation of an iron hypophosphite protective film on the contacting surfaces as an AW agent is limited to low-load conditions. While some studies have also shown that under high loads, phosphate esters partially hydrolyze, leading to the formation of an organic iron phosphate layer, which inhibits direct metal-to-metal contact between the rubbing interfaces [25]. Hence, these studies demonstrated that the behaviour of phosphorus-containing additives is influenced by specific operational sliding parameters (load, speed, and temperature) [24,25]. The polar component of the surface free energy (SFE) of the steel decreases as the surface becomes covered by hydrocarbon-rich fragments of decomposed phosphate esters [26,27]. This reduction in surface free energy (SFE) improves wettability and compatibility with the base oil under high-load conditions, reducing interfacial tension and promoting film cohesion [28]. Zhao et al. [29] demonstrated that the phosphate ester film with reduced surface polarity enhances compatibility with polyalkylene glycol (PAG) base oil, improving the cohesion of the tribofilm composed of $FePO_4$ and oxide layers and AW properties. Furthermore, the higher polarity of phosphate esters promotes excessive adsorption on metal surfaces, resulting in hydrolysis (formation of phosphoric acid) and causing pitting and corrosive wear [30]. Therefore, a moderate polarity is essential to enhance wetting, adsorption kinetics, and tribofilm stability to preserve AW properties.

Additionally, acidic phosphate esters exhibit higher activity, stronger anti-rust (AR) capacity on metal surfaces, and superior extreme pressure and AW performance [26,30]. Nevertheless, they demonstrate fast phosphorus depletion. To solve the problem of poor corrosion resistance caused by the high acidity of acidic phosphate esters, they can be converted into amine salts. This modification achieves extreme pressure and wear resistance while reducing corrosion [31]. In this study, ionic liquids based on the phosphate amine salts (IL-NPAS), a type of multifunctional lubricating oil additive with both AR and AW properties, have been derived. At the same time, the functional groups of phosphate amine salts have strong chemical activity and can easily form low-shear layers that stick to metal surfaces [32]. The layered structure of phosphate produced during friction also ensures its lubricity [33]. Among fatty acid phosphate ester AR and AW agents, King's AW-6110

outperforms comparable products on the market and is already a leader in the high-end lubricant industry [34].

In this investigation, we have successfully addressed the issues described earlier by synthesizing four different types of ammonium phosphate salts. These distinctive additives were developed with the goal of improving the properties of AW and AR. The AR and AW properties of ammonium phosphate salts are compared to commercial AW-6110, a competitor. This approach allows us to show the industrial feasibility of currently synthesized additives. Oil-based lubricating additives, as well as their AR and AW, were thoroughly studied. This research reveals the key mechanism of the protective tribolayer on the worn interfaces. To illustrate the wear modes and main tribofilm formation mechanism, scanning electron microscopy (SEM), X-ray photoelectron spectroscopy (XPS) and time-of-flight secondary ion mass spectrometry (TOF-SIMS) were employed to examine the chemical composition and characteristics of the wear scar. Additionally, the AW properties of the developed oil-based lubricating additive are discussed. Eventually, the current results will be advantageous for the future advancement of lubricating oils that decrease friction and improve the durability of the tribopair in mechanical applications by providing new ideas for the molecular design of AR and AW additives.

2. Materials and Methods

2.1. Materials, Synthesized, and Characterizations

In this investigation, 150 SN oil was selected as the baseline lubricant to evaluate the lubrication performance of a novel ionic liquid based on a phosphate ammonium salt, designated herein as IL-NPAS. To offer the suitability of the IL-NPAS additive, a commercial additive (referred to as AW6110) was used to compare its lubrication performance with the synthesized additive. AW6110 was sourced from King Industries, Dalian Mingruida Technical Consulting Co., Ltd., Dalian, China. As mentioned by the manufacturer in the specifications [35], AW6110 additive includes 8.0% phosphorus and 1.8% nitrogen in its composition. Table 1 lists the reagents employed in the synthesis of the IL-NPAS additive. The molecular structure of the synthesized additive was characterized using a Bruker AVANCE III HD 400 MHz superconducting nuclear magnetic resonance (NMR) equipped with a micro TOF-Q II system, enabling both qualitative and quantitative structural analysis.

Table 1. Reagents used in the synthesis of ammonium phosphate salt additives.

Reagent	Manufacturer	Purity/%
Dodecylamine	Chemical Regents	99
Dibutyl phosphate	Chemical Regents	99
N,N-dimethylhexadecylamine	Chemical Regents	98
Diisooctyl phosphate	Chemical Regents	95
150 SN	PetroChina	96
Ethanol	Chemical Regents	99

The synthesis of the IL-NPAS involved four processes to obtain four samples, as below: Sample 1 was prepared by combining equimolar amounts of dodecylamine and dibutyl phosphate in a 100 mL round-bottom flask. The solution was heated at 80 °C for 2 h to confirm a complete reaction, then cooled to room temperature. Sample 2 was prepared by combining equimolar amounts of dodecylamine and diisooctyl phosphate using a process identical to that of Sample 1. Sample 3 was produced by reacting equimolar amounts of N,N-dimethylhexadecylamine and dibutyl phosphate under the same conditions. Sample 4 was prepared using the same method as Sample 1, with equimolar quantities of N,N-dimethylhexadecylamine and diisooctyl phosphate. Finally, the novel additive was

formulated by combining samples 1, 2, 3, and 4 in a 1:1:1:1 mass ratio. After that, this mixture was heated and maintained at 70 °C for 2 h to confirm homogeneity. The reaction conditions facilitate the synthesis via a regulated heat reaction between the phosphate ester and the main amine [36,37]. Figure 1 shows the synthesis process and molecular structure of the synthetic IL-NPAS additive during the four stages of its manufacture. The primary motivation for manufacturing IL-NPS additive is to provide a halogen-free oil additive that reduces toxicity and offers high biodegradability compared to commercial additives. These features are compatible with environmental requirements for lubricant formulations.

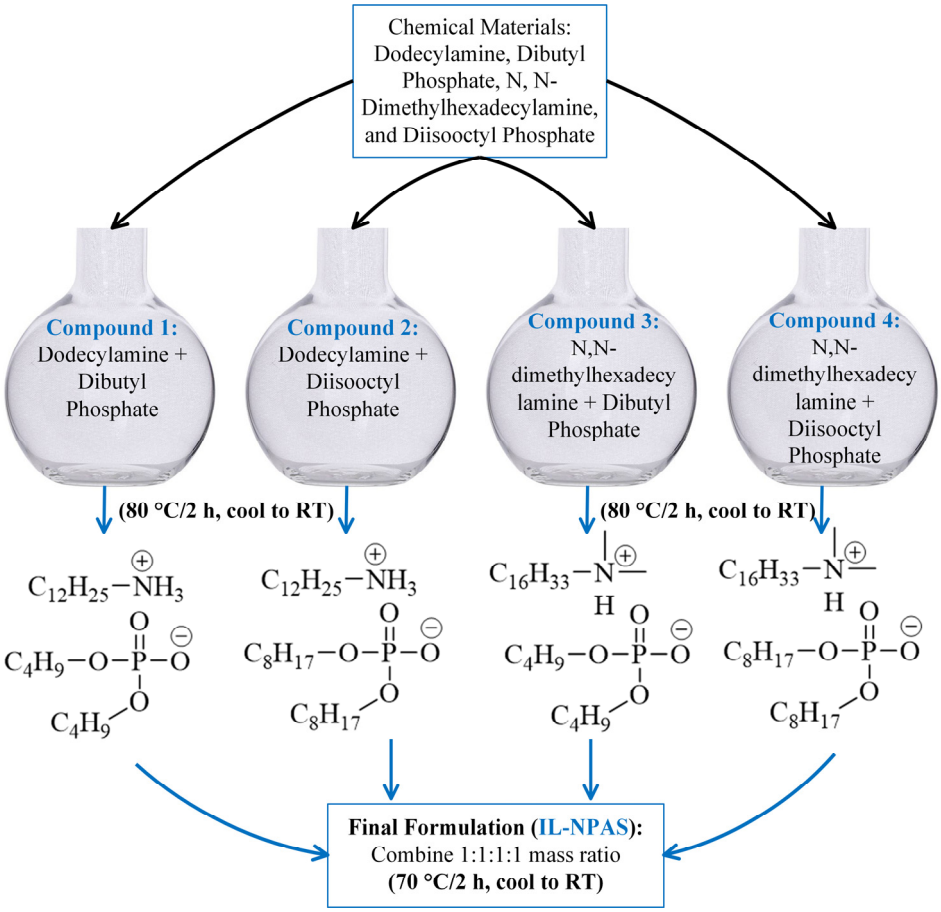

Figure 1. Synthesis process and molecular structure of the synthetic IL-NPAS compounds during the four stages of its synthesis.

The molecular structures of the synthesized IL-NPAS compounds were characterized using ^{1}H, ^{13}C, and ^{31}P nuclear magnetic resonance (NMR) spectroscopy. These spectra sufficiently demonstrate that our ammonium phosphate is successfully synthesized. The detailed analysis of the NMR data is presented below.

In compound 1: ^{1}H NMR (400 MHz, $CDCl_3$) δ: 8.58 (s, 3H), 3.78 (t, J = 8.0 Hz, 4H), 2.75 (s, 2H), 1.69–1.53 (m, 6H), 1.40–1.23 (m, 21H), 0.92–0.84 (m, 9H). ^{13}C NMR (100 MHz, $CDCl_3$) δ: 65.37, 65.31, 39.62, 33.07, 32.99, 32.03, 29.78, 29.78, 29.44, 27.91, 27.10, 22.81, 19.17, 14.22, 13.94. 31P NMR (162 MHz, $CDCl_3$) δ: 0.34 (s). m/z (ESI, positive ion) calc.: 186.2222, found: 186.2229 $[C_{12}H_{28}N]^{+}$, m/z (ESI, negative ion) calc.: 209.0943, found: 209.0946 $[C_8H_{18}PO_4]^{-}$.

In compound 2: ^{1}H NMR (400 MHz, $CDCl_3$) δ: 8.58, sH, 3.78 (t, J = 8.0 Hz, 4H), 2.75 (s, 2H), 1.69–1.53 (m, 6H), 1.41–1.24 (m, 34H), 0.92–0.85 (m, 9H). ^{13}C NMR (100 MHz, $CDCl_3$) δ: 65.43, 65.37, 39.64, 33.05, 32.98, 32.06, 29.85, 29.80, 29.50, 29.46, 27.11, 22.83, 19.17, 14.25, 13.95. ^{31}P NMR (162 MHz, $CDCl_3$) δ: 0.25 (s). m/z (ESI, positive ion) calc.: 186.2216,

found: 186.2220 $[C_{12}H_{28}N]^+$, *m*/*z* (ESI, negative ion) calc.: 321.2195, found: 321.2210 $[C_{16}H_{34}PO_4]^-$.

In compound 3: ^{1}H NMR (400 MHz, $CDCl_3$) δ: 4.42 (s, 4H), 3.81–3.77 (m, 8H), 3.57 (t, J = 8.0 Hz, 4H), 3.30 (s, 12H), 1.79–1.69 (m, 4H), 1.53–1.19 (m, 88H), 0.89–0.85 (m, 30H). ^{13}C NMR (100 MHz, $CDCl_3$) δ: 68.72, 68.66, 65.78, 57.19, 50.61, 40.34, 40.26, 32.07, 30.09, 29.86, 29.81, 29.76, 29.62, 29.51, 29.11, 26.41, 23.35, 23.20, 22.83, 14.22, 11.04. ^{31}P NMR (162 MHz, $CDCl_3$) δ: 0.26 (s). *m*/*z* (ESI, positive ion) calc.: 242.2848, found: 242.2840 $[C_{16}H_{36}N]^+$, *m*/*z* (ESI, negative ion) calc.: 209.0943, found: 209.0949 $[C_{88}H_{18}PO_4]^-$.

In compound 4: ^{1}H NMR (400 MHz, $CDCl_3$) δ: 8.58 (s, 3H), 3.78 (t, J = 8.0 Hz, 4H), 2.75 (s, 2H), 1.69–1.53 (m, 6H), 1.40–1.23 (m, 21H), 0.92–0.84 (m, 9H). ^{13}C NMR (100 MHz, $CDCl_3$) δ: 65.37, 65.31, 39.62, 33.07, 32.99, 32.03, 29.78, 29.78, 29.44, 27.91, 27.10, 22.81, 19.17, 14.22, 13.94. ^{31}P NMR (162 MHz, $CDCl_3$) δ: 0.34 (s). *m*/*z* (ESI, positive ion) calc.: 242.2848, found: 242.2840 $[C_{16}H_{36}N]^+$, *m*/*z* (ESI, negative ion) calc.: 209.0943, found: 209.0949 $[C_8H_{18}PO_4]^-$.

The formulated lube oils consisted of 150 SN oil blended with IL-NPAS at concentrations of 0.1 wt% and 0.5 wt%. Generally, organic additives exhibit their most cost-effective friction-reducing performance at concentrations ranging from approximately 0.25 to 1 wt% [38]. Additionally, the manufacturer (King Industries) specifies that the recommended dosage of the AW6110 additive in oils for various industrial applications ranges from 0.1 to 0.5 wt% [35]. Accordingly, the present study employed concentrations of 0.1–0.5 wt% for both the IL-NPAS and AW6110 additives. The kinematic viscosity and viscosity index of the studied oil additives and lube oils are summarized in Table 2. The kinematic viscosity measurements of the commercial additive (AW6110) showed values close to those specified by the manufacturer [35]. Comparing the viscosity values of the additives, the designed additive (IL-NPAS) offered a 4.4% lower value at 40 °C compared to the AW6110 additive. However, the viscosity values at 100 °C for both additives were nearly identical. The measurements indicated a slight reduction in viscosity when the oil additives are incorporated in 150 SN oil. The formulated oils did not show significant differences that affect the rheological behaviour. Furthermore, the tested oils also showed a nearly similar viscosity index, which is calculated according to the ASTM D2270 standard.

Table 2. Measurements of kinematic viscosity of lube oils and their viscosity index values.

Lubricant Sample Name	Kinematic Viscosity (mm^2/s)		Viscosity Index
	@ 40 °C	@ 100 °C	
IL-NPAS	469.77	35.58	109
AW6110	491.57	35.32	114
Base oil (150 SN)	32.730	5.6678	112.9
150 SN oil + 0.5 wt% IL-NPAS	30.741	5.4142	111.1
150 SN oil + 0.1 wt% IL-NPAS	30.935	5.4353	111.0
150 SN oil + 0.5 wt% AW6110	30.966	5.4400	111.1
150 SN oil + 0.1 wt% AW6110	30.859	5.4308	111.3

2.2. Tribological Tests

Tribological evaluations of the synthesized IL-NPAS additive and the commercial AW6110 additive in 150 SN base oil were systematically performed using an Optical SRV-IV Germany tribometer. The test parameters are summarized in Table 3. Friction tests were performed at 25 °C and 100 °C to simulate actual operating circumstances in automotive systems [39]. The lower temperature (25 °C) suggests cold-start conditions, facilitating measurement of AW performance without considerable thermal impact. The higher temperature (100 °C) reflects a steady-state operational case in engine crankcases and gearboxes. The tribological contact configuration consisted of an AISI 52100 steel

ball (10 mm diameter, hardness ≈ 60 ± 2 HRC) sliding against a flat AISI 52100 steel disc (24 mm diameter, 8 mm height, hardness 58–62 ± 2 HRC). The disc had an initial average surface roughness (Sa) of 0.036 µm before the friction tests. Most tribological research and standard testing protocols use AISI 52100 steel as rubbing friction samples. It is especially friction testing featuring steel-on-steel contact that simulates actual material in transmission components (bearings and gears) for various mechanical/tribological systems. To ensure reproducibility, each frictional trial was conducted in duplicate under identical conditions, and the reported results represent the average coefficient of friction (COF) and average wear volume.

Table 3. The tribological test conditions.

Parameter (Unit)	Value
Tribopair materials	Steel–steel Contact
Load (N)	200
Frequency (Hz)	50
Temperature (°C)	25/100
Amplitude (mm)	1
Duration test (min)	30

After performing the rubbing tests, the surface 3D profilometer Bruker-NPFLEX was applied to measure the wear volume of the disc wear scars. The surface morphology and chemical composition of the wear spot surfaces were analyzed by SEM and EDS (model: FEG Quanta 350). The element valence and binding energy on the lubricating tribolayer were identified using XPS (model: PHI-5702 multipurpose). Additionally, the chemical composition of the tribofilm formed on the rub surface was characterized via a PHI Nano-TOF time-of-flight secondary ion mass spectrometer (TOF-SIMS).

3. Results and Discussion

3.1. Tribological Properties

To highlight how the IL-NPAS and AW6110 additives affect friction in base oil (150 SN), it is important to show how the COF behaviour during the sliding time of the experiment. Figure 2a illustrates the variation in COF behaviour of lubricants containing IL-NPAS and AW6110 additives at concentrations of 0.5 and 0.1 wt% at a load of 200 N and a sliding frequency of 50 Hz under room temperature (25 °C) conditions. From Figure 2a, it can be clearly seen that as time increases, the COF of 150 SN continues to slightly increase. Approximately 200 s marks a sudden increase in the COF of the lubricant containing 0.1 wt% AW6110. The oil formulated with 0.1 wt% IL-NPAS exhibited superior friction-reducing performance compared to the oil containing 0.1 wt% AW6110 during the initial half of the friction test. Thereafter, a sudden and sharp increase in the COF, indicative of a seizure event, occurred in the middle of the experiment. Hence, the COF trends of both formulated oils were nearly identical, like the base oil behaviour. These observations highlight the inability of low concentrations (0.1 wt%) of both IL-NPAS and AW6110 additives to prevent seizure phenomena under the tested conditions. While the COFs of the 0.5 wt% IL-NPAS and 0.5 wt% AW6110 additives show more stability during sliding time. Remarkably, the results showed that the 0.5 wt% IL-NPAS and 0.5 wt% AW6110 additives provided a lower COF of around 0.12, presenting nearly similar COF trends. The average COF was reduced by 34–36% for both the 0.5 wt% IL-NPAS and 0.5 wt% AW6110 formulations, compared with the baseline oil. The reduction can be attributed to the increase in the chain length of the phosphate ammonium additive and the thickness of the adsorption film at room temperature [40]. The results revealed that the additives (IL-NPAS and AW6110) at the

higher concentration were remarkably effective in reducing friction, and the performance of the two additives was almost identical.

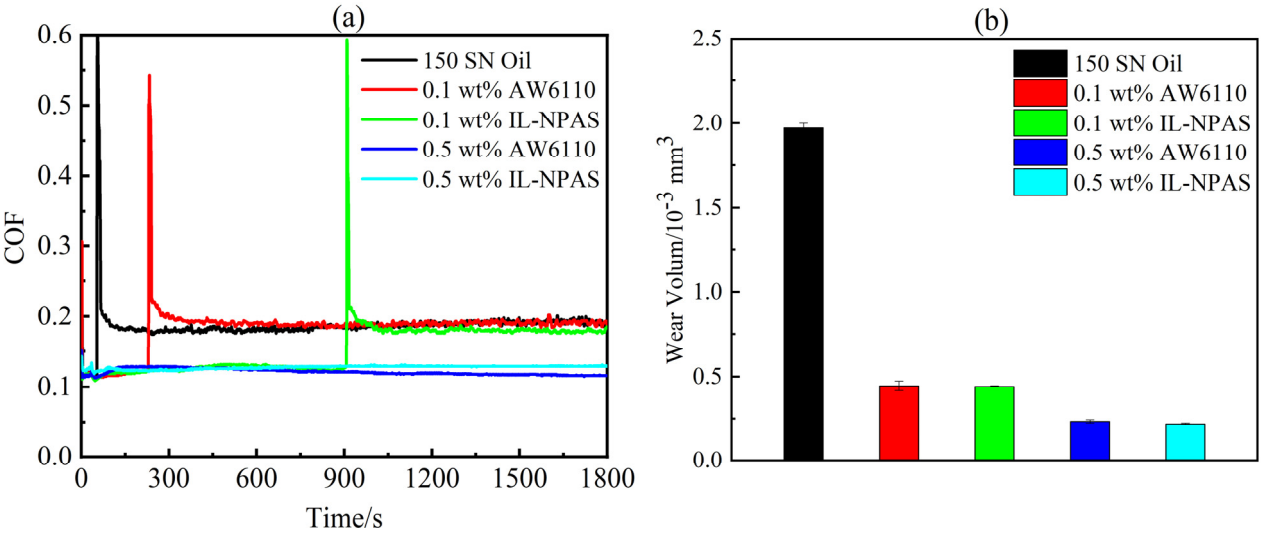

Figure 2. COF behaviour versus sliding time (**a**) and wear volume of the disc (**b**) for tested oil additives at 200 N and 50 Hz under low temperature (25 °C).

Additionally, a comparison of disc wear volumes under lubrication with the novel IL-NPAS and commercial AW6110 additives is shown in Figure 2b. The results indicated that both oils containing 0.1 wt% of IL-NPAS and AW6110 additives exhibited similar wear resistance. These oils containing 0.1 wt% additives reduced wear volume by 70% compared to the 150 SN base oil. Thereby, the AW behaviour of the IL-NPAS and AW6110 additives shows a trend consistent with that of the COF results. The results iullstred nearly identical wear volumes for both formulated oils at the studied concentrations, indicating equivalent AW performance. Remarkably, the results indicated that the wear volume of the disc lubricated with 0.5 wt% IL-NPAS in 150 SN oil was reduced by 80–85% compared to that of the baseline 150 SN oil. In the 150 SN basic lubricant, the higher wear volume is attributed to the absence of active elements such as P and N elements, as well as the lack of long alkyl chains [34].

To illustrate the role of the novel IL-NPAS additive in high temperature, Figure 3 exhibits the variation curve of the COF of the lubricant containing various oil additives during sliding time, as well as the wear volume of the steel disc surface under 100 °C. From Figure 3a, it can be clearly seen that as time increases, the COF suddenly increases for formulated oils with lower concentration (0.1 wt%) between 600 and 900 s of the sliding, demonstrating the occurrence of seizure phenomenon because of metal-to-metal contact. Moreover, the instability noted in the COF behaviours of formulated oils at low concentrations may be related to more production of wear debris as a third body between the rubbed surfaces. This behaviour reflects deterioration of the worn surfaces or gradual depletion of lubrication. Notably, the COFs of 0.5 wt% AW6110 and 0.5 wt% IL-NPAS showed a reduction of 40–45% compared to neat lubricant. This reduction is mainly owing to the increase in the chain length of the P element and the formation of the adsorption film at 100 °C [19]. Hence, the higher concentration of IL-NPAS and AW6110 additive is more effective for steel/steel lubrication at 100 °C. Furthermore, the COF behaviours of the additives are more stable during the friction test at 100 °C.

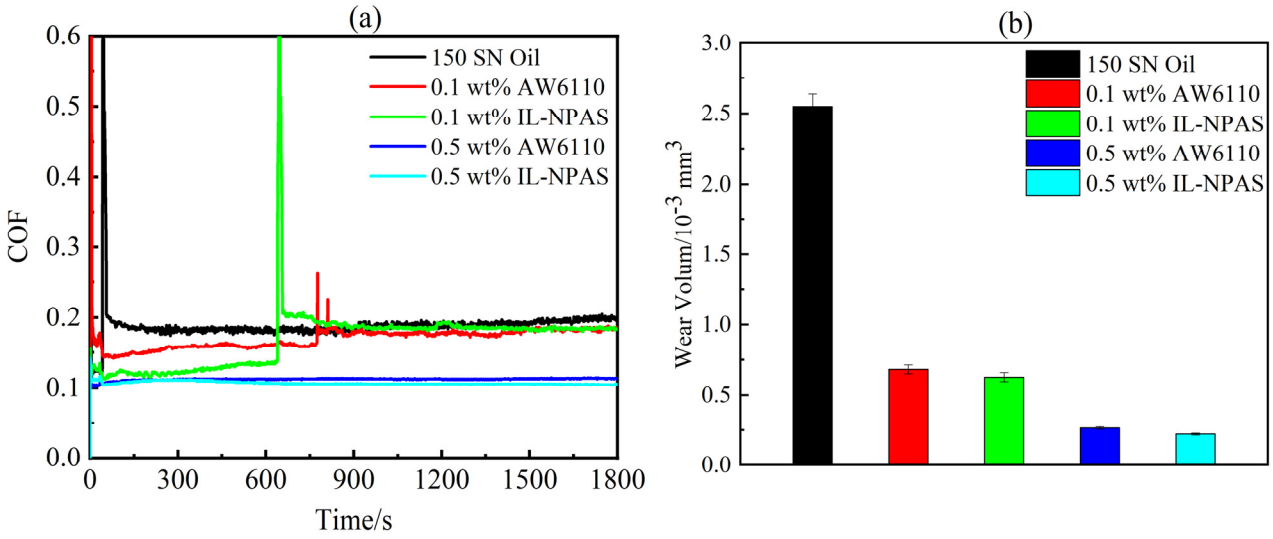

Figure 3. COF behaviour versus sliding time (**a**) and wear volume of the disc (**b**) for investigated oil additives under 100 °C temperature at 200 N and 50 Hz.

At 100 °C (Figure 3b), the results illustrated that the wear volume for various oil additives decreased compared to 150 SN oil. The lubricants containing a low concentration (0.1 wt%) of IL-NPAS and AW 6110 additives revealed a 72% improvement in AW properties compared with 150 SN base oil. The IL-NPAS additive behaved similarly to the commercial AW6110 addition in terms of its AW properties at studied concentrations. It is noteworthy that the AW6110 and IL-NPAS additives with high concentrations (0.5 wt%) showed the highest AW improvement, up to 90%, compared with base oil. This improvement in AW properties is related to the IL-NPAS additive, which includes active N and P elements and longer alkyl chains in the lubricant [41,42]. At 100 °C, these elements make it easy to form physical adsorption layers on the surfaces that are rubbing against each other [43]. This makes them better for super-lubrication and gives them the best AW properties. Xiang et al. [44] illustrated that the chemisorption is facilitated by π-electron donation from aromatic or heteroatom components of the ammonium-based IL, accelerating tribofilm formation on the steel interfaces. This mechanism improves COF reduction and wear resistance under the boundary lubrication regime. Additionally, the AW6110 addition is characterized by its polar phosphate groups esterified with long-chain alcohols and neutralized with amines for improved thermal stability and decomposes under frictional heating to produce reactive phosphorus species that chemisorb on steel substrates [38,45]. Ewen et al. [46] indicated that the decomposition mechanisms of phosphate esters primarily include the breaking of C-O and P-O bonds. As a result, the AW6110 addition enhances the level of polyphosphates, pyrophosphates, and iron phosphates within the tribofilm, which increases wear resistance [34].

3.2. Morphological Characterization

This section provides an explanation of the wear patterns to illustrate the mechanisms that result in the improved AW properties and reduced COF of the AW6110 and IL-NPAS oil additives. Figure 4 shows the three-dimensional profilometer, length, and width of the wear marks on the wear disc scar, which was oiled with 150 SN oil, AW6110, and new IL-NPAS additives at 0.1 wt% and 0.5 wt% under the above conditions mentioned in Section 3.2. The results revealed that lubrication with 150 SN oil produced the largest wear scar. This scar further increased at a temperature of 100 °C, showing a wear volume of 2.5×10^{-3} mm^3 (Figure 3b), compared to 2×10^{-3} mm^3 at 40 °C (Figure 2b). It is noteworthy that in the case of lubrication with oil containing 0.5 wt% AW6110 at a temperature of 100 °C,

the wear scar was larger in dimensions (Figure 4d1) when compared to the wear scar at a temperature of 25 °C (Figure 4d). In contrast, Figure 4e,e1 illustrates that the disc lubricated by the 0.5 wt% IL-NPAS additive has the least noticeable wear marks when compared to the samples lubricated by 150 SN oil and AW6110 additive. Additionally, the absence of the sharpest edges of wear scars (Figure 4e,e1) suggests a more uniform wear process compared to base oil and oils containing a lower concentration of additives. This observation is attributed to the formation of a protective tribofilm that incorporates wear debris, thereby reducing the detachment rate of wear particles. The decrease in wear is mainly attributed to the elongated alkyl chains seen in the molecular composition of the phosphate ammonium in the IL-NPAS additive [47], which corresponds to the exceptional tribological characteristics demonstrated in Figures 2 and 3. Additionally, the worn disc surface has small abrasion marks, minor scratches, and abrasions. As a result, these observations indicate that the synthesized IL-NPAS additive at 0.5 wt% has higher AW properties for lubricating steel-steel tribopair.

Figure 5 presents SEM images of the wear scars on disc surfaces tested under a load of 200 N, at 25 °C, and a frequency of 25 Hz. The scar produced with the base 150 SN oil is severe wear, featuring irregular edges, extensive material delamination, and localized accumulations of wear debris (Figure 5a,a1). The rubbing surfaces lubricated with 0.1 wt% AW6110 or 0.1 wt% IL-NPAS exhibit pronounced surface rub marks along with widespread material delamination and peeling (Figure 5b1,c1). These morphological characteristics suggest partial material removal and the formation of microwelds of wear particles on the worn surface, demonstrating the dominance of the adhesive wear pattern. Interestingly, wear scars generated with the higher additive concentration (0.5 wt%) of either IL-NPAS or AW-6110 display only shallow ploughing grooves and a relatively smooth surface, devoid of peeling or tearing features (Figure 5d1,e1). This morphology is attributed to favourable tribochemical reactions, wherein the additives interact with the steel surface to form a protective tribofilm that effectively suppresses adhesive wear mechanisms. Briefly, the morphological analysis indicates that both additives, at 0.5 wt%, significantly enhance the adhesive wear resistance of the steel tribopair.

Under high temperature, Figure 6 shows the morphology images of the wear scar of the disc surface lubricated with oil additives under 200 N, 100 °C, and 50 Hz conditions. The disc surface lubricated with base oil alone exhibited irregular edges, severe peeling, and debris in some areas on the worn surfaces (Figure 6a,a1). These observations demonstrate that the wear mode is characteristic of both adhesive and abrasive wear modes. The wear tracks on the disc interface lubricated with 0.1 wt% AW6110 and 0.1 wt% IL-NPAS additives revealed significant areas of peeling, wear spots, deep gouges, and debris on the rubbing surface. This damage is primarily indicative of adhesive wear under 100 °C temperature, accompanied by abrasive wear. As shown in Figure 6b1,c1, the worn surfaces exhibit scratches characteristic of third-body wear, resulting from wear debris becoming entrapped between the sliding interfaces. At elevated temperatures, this mechanism is significantly aggravated because of the oxidation and the formation of abrasive particles. Furthermore, high temperatures diminish the effectiveness of the lubricant film, leading to increased direct contact between surface asperities and consequently increasing abrasive wear. Notably, the wear spots on the disc lubricated by 0.5 wt% IL-NPAS additive are relatively smooth, with only plough grooves. Although minor pitting wear is observed in some regions, the results demonstrate that the rubbing surface degradation at high temperature is markedly more severe than that under ambient temperature. Meanwhile, the IL-NPAS addition at various concentrations (0.1 and 0.5 wt%) is more suitable as a high-temperature lubrication additive for steel/steel friction interfaces.

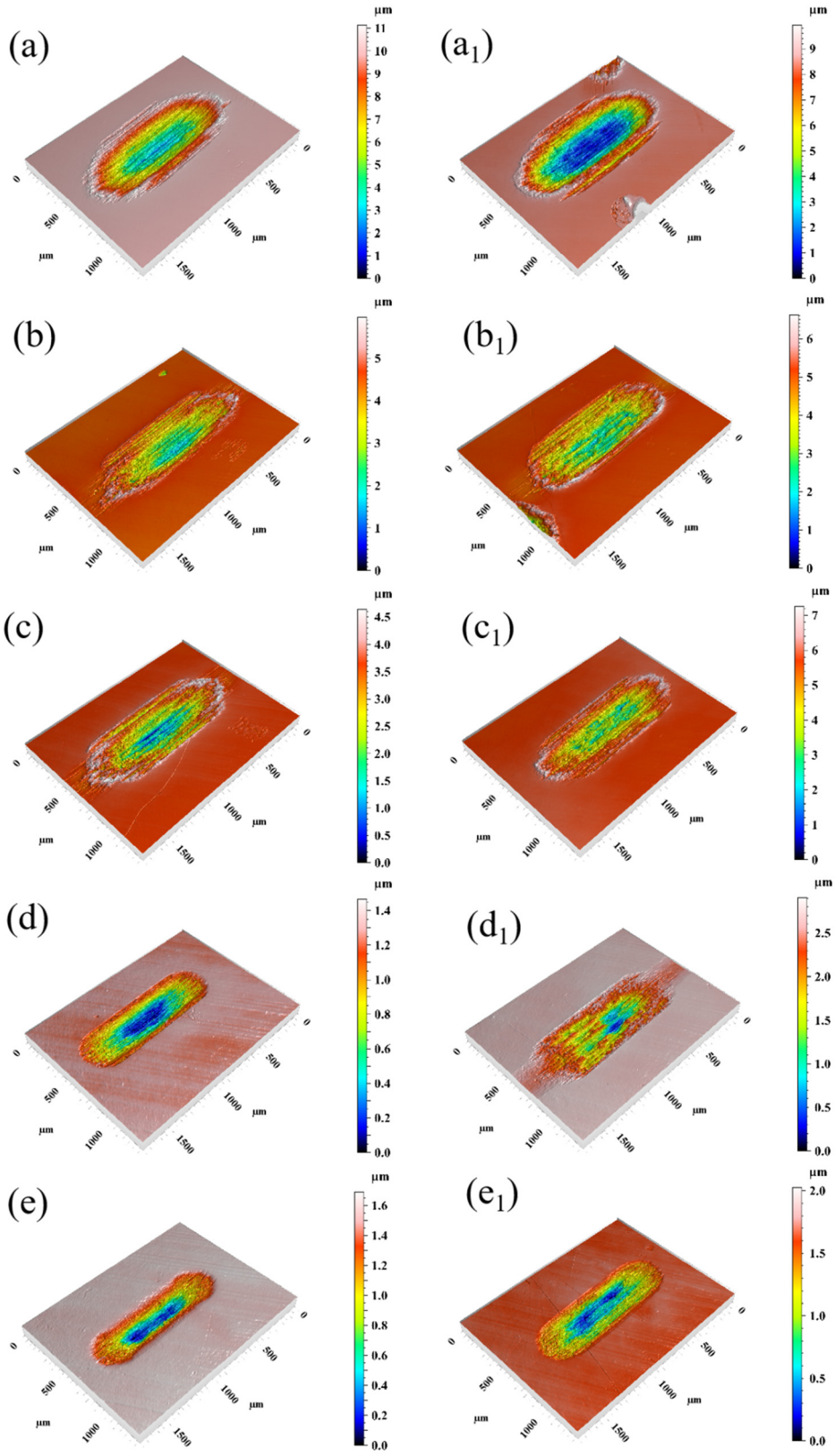

Figure 4. Three-dimensional wear scar morphologies of the disc surface oiled with 150 SN neat oil (**a**,**a**$_1$); 0.1 wt% AW6110 (**b**,**b**$_1$); 0.1 wt% IL-NPAS (**c**,**c**$_1$); 0.5 wt% AW6110 (**d**,**d**$_1$); 0.5 wt% IL-NPAS (**e**,**e**$_1$). (**a**–**e**: at 25 °C, **a**$_1$–**e**$_1$: at 100 °C).

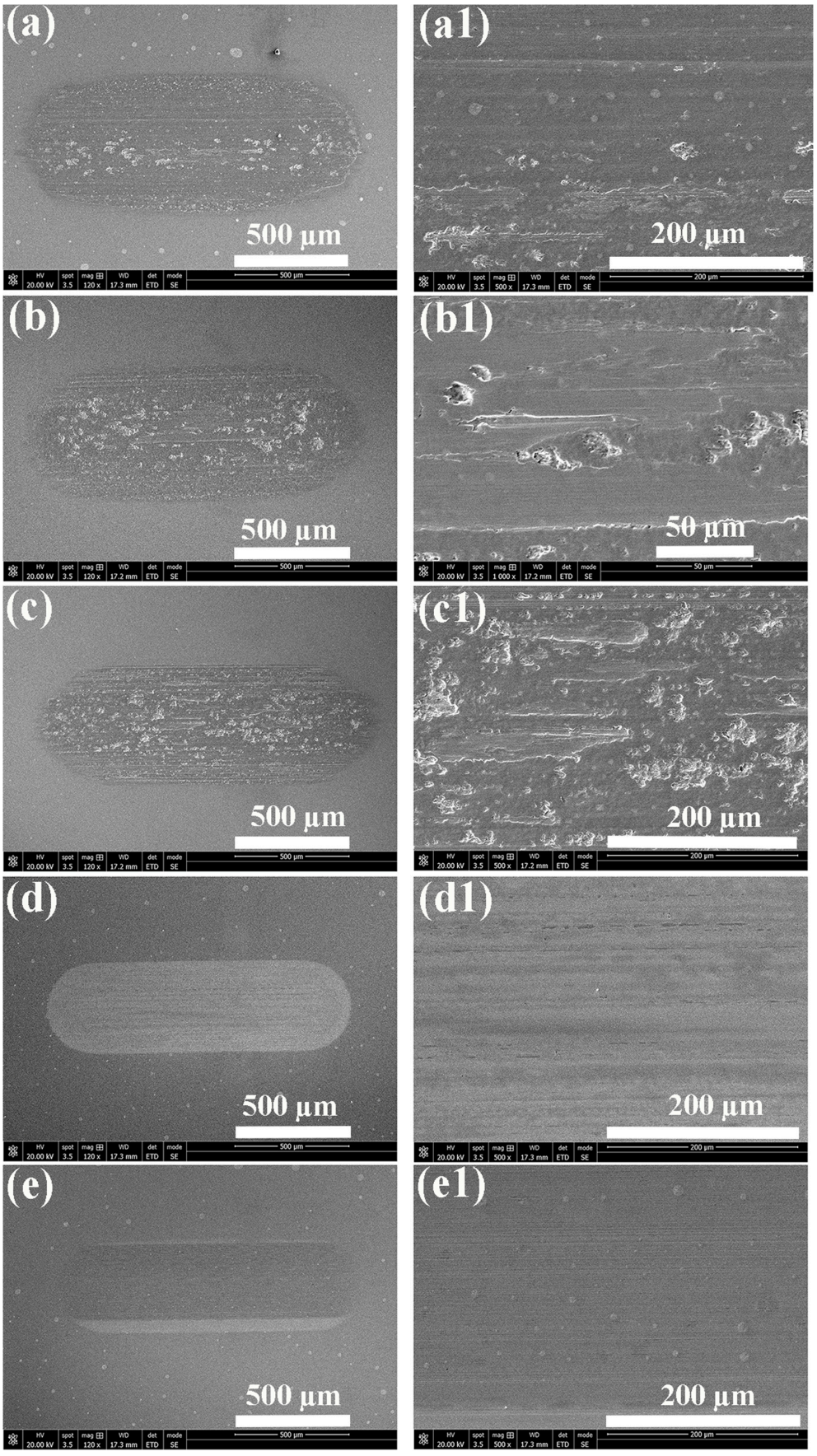

Figure 5. SEM images of the wear track for disc at 200 N and 50 Hz under 25 °C temperature: 150 SN oil (**a**,**a**$_1$); 0.1 wt% AW6110 (**b**,**b**$_1$); 0.1 wt% IL-NPAS (**c**,**c**$_1$); 0.5 wt% AW6110 (**d**,**d**$_1$); 0.5 wt% IL-NPAS (**e**,**e**$_1$).

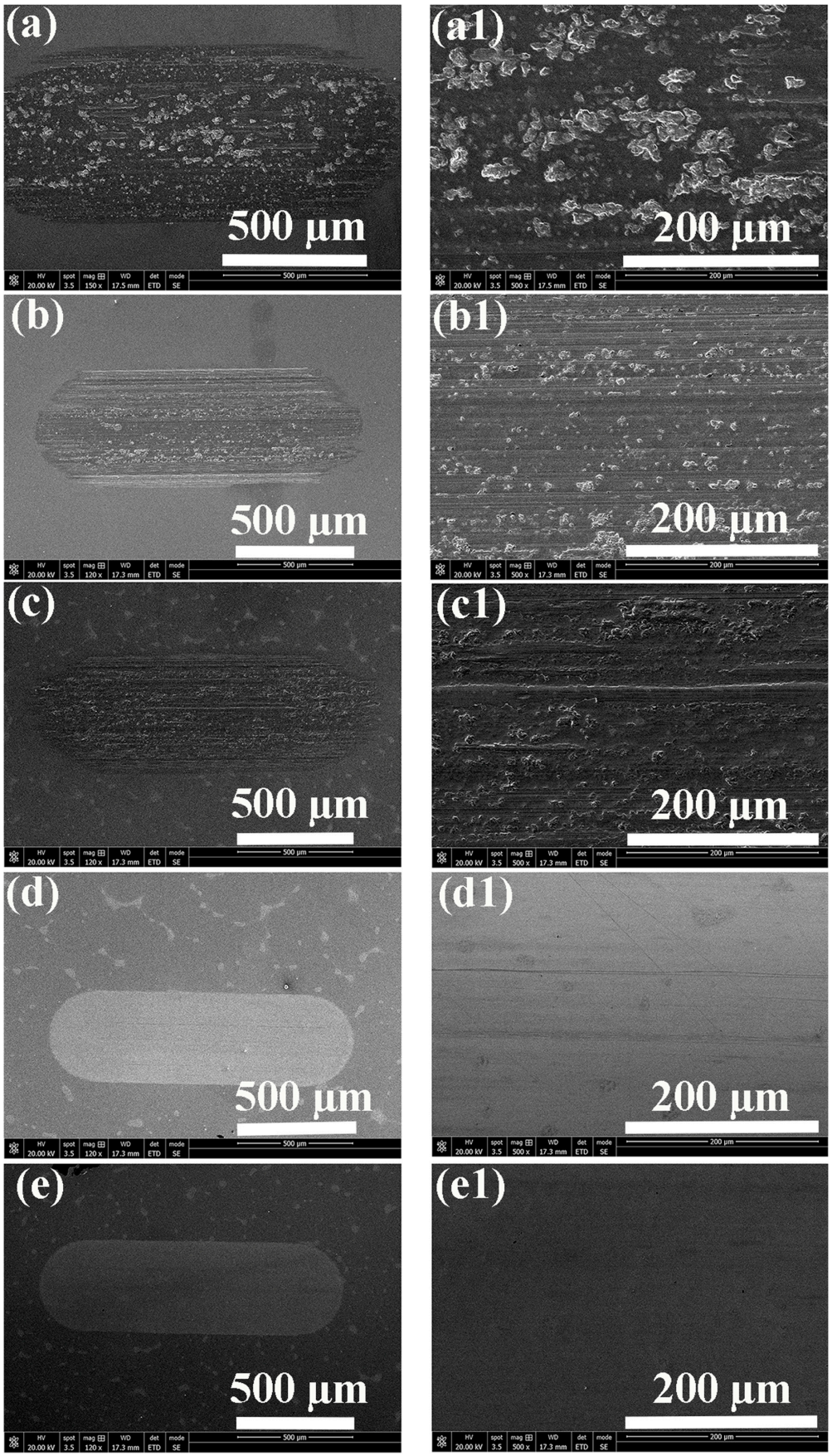

Figure 6. SEM images of the rub disc track at 200 N and 50 Hz under 100 °C temperature: 150 SN oil (**a**,**a**$_1$); 0.1 wt% AW6110 (**b**,**b**$_1$); 0.1 wt% IL-NPAS (**c**,**c**$_1$); 0.5 wt% AW6110 (**d**,**d**$_1$); 0.5 wt% IL-NPAS (**e**,**e**$_1$).

3.3. Wear Resistance Mechanism

To elucidate the wear resistance mechanism, XPS was performed on the rub disc surfaces oiled by the IL-NPAS additive. Figure 7 presents the HR-XPS spectra of the rub scar lubricated with 0.5 wt% IL-NPAS addition. The characteristic binding energy positions of the C 1s, O 1s, N 1s, P 2p, and Fe 2p peaks remain consistent under both room temperature (RT, 25 °C) and elevated temperature (HT, 100 °C) conditions. This similarity suggests that the underlying tribochemical reactions are fundamentally similar under various temperatures. The energy spectrum of Fe2p offers that the major characteristic peaks of Fe correspond to binding energies of 710.8, 713.8, 723.7, and 726.3 eV, corresponding to FeO, Fe_2O_3, FeOOH, and iron phosphate, respectively [48,49]. The characteristic element spectrum of the worn surface after friction presents that the electron binding energy of N1s is approximately 400.3–399.7 eV. It is important to note that under high-temperature conditions, the peak intensity of N1s is higher than that observed at room temperature. This note suggests that tribo-chemical reactions are more likely to occur at 100 °C, leading to the formation of thicker boundary lubrication tribolayers. The result aligns with the findings from the TOF-SIMS analysis (Figure 8). In the P 2p spectrum, the presence of phosphate species is evident from the characteristic peaks observed on the rub surface after friction, which are further corroborated by the O 1s spectral features, indicating that phosphorus primarily exists in the form of phosphate [50,51]. XPS analysis reveals that phosphate ammonium salt additives function effectively as lubricants in steel-on-steel contacts by participating in tribochemical reactions during friction events. These reactions lead to the formation of a boundary tribofilm composed of iron oxides (FeO, Fe_2O_3, FeOOH) and iron phosphate. This tribofilm acts as a protective layer, significantly reducing the COF and improving the wear resistance property of the rubbing interfaces. In conclusion, the IL-NPAS additive demonstrates superior lubrication performance and is particularly well-suited as a high-temperature lubricant for steel-on-steel contacts, as illustrated in Figure 3.

Furthermore, the chemical composition within the rub scar of the disc was investigated using TOF-SIMS analysis to show the tribofilm mechanism. Figure 8 presents the TOF-SIMS spectrum of the steel disc surface oiled by 0.5 wt% IL-NPAS additive. The TOF-SIMS positive ion spectra at room temperature and high temperature indicate that the CH_3^+, $C_2H_3^+$, $C_2H_5^+$, $C_3H_7^+$, and $C_4H_9^+$ on the rub spot originate from cations in the phosphate ammonium compound. This finding indicates that, during the friction process, the alkyl chains of the cations in the phosphate ammonium-based additive undergo thermal or mechanical degradation, yielding smaller molecular fragments [52]. In addition, the detection of high-intensity Fe ions and $C_xH_y^+$ signals confirms the presence of inorganic salts or oxides [53]. The negative-ion TOF-SIMS spectrum of the steel surface reveals the presence of C^-, CH^-, O^-, OH^-, CN^-, CNO^-, PO_2^-, PO_3^-, and HPO_3^- fragments, which originate from tribochemical reactions between the anionic components of the phosphate ammonium additive and the steel substrate. The positive and negative ion spectra show that the ion intensity on the disc rub scar is higher after high-temperature lubrication compared to room temperature lubrication conditions. These results indicate that the friction process is more intense under high-temperature conditions, making it easier to obtain frictional chemical reaction products and generate stable boundary lubrication films, thereby improving the lubrication performance of steel tribopair lubricated by IL-NPAS additive.

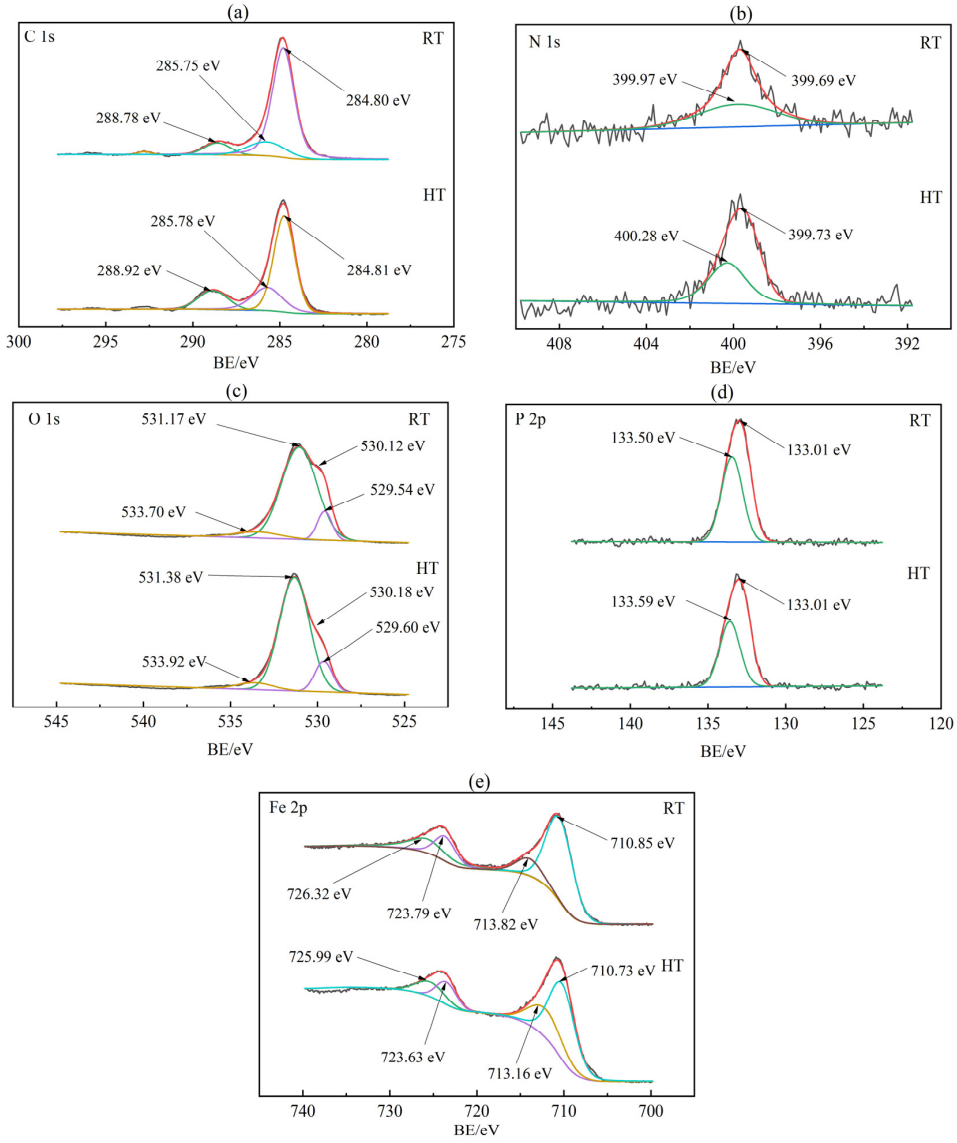

Figure 7. HR-XPS analysis of C1s (**a**), N1s (**b**), O1s (**c**), P2p (**d**), and Fe2p (**e**) on the rub disc spot oiled with 0.5 wt% IL-NPAS additive at 25 °C and 100 °C temperatures.

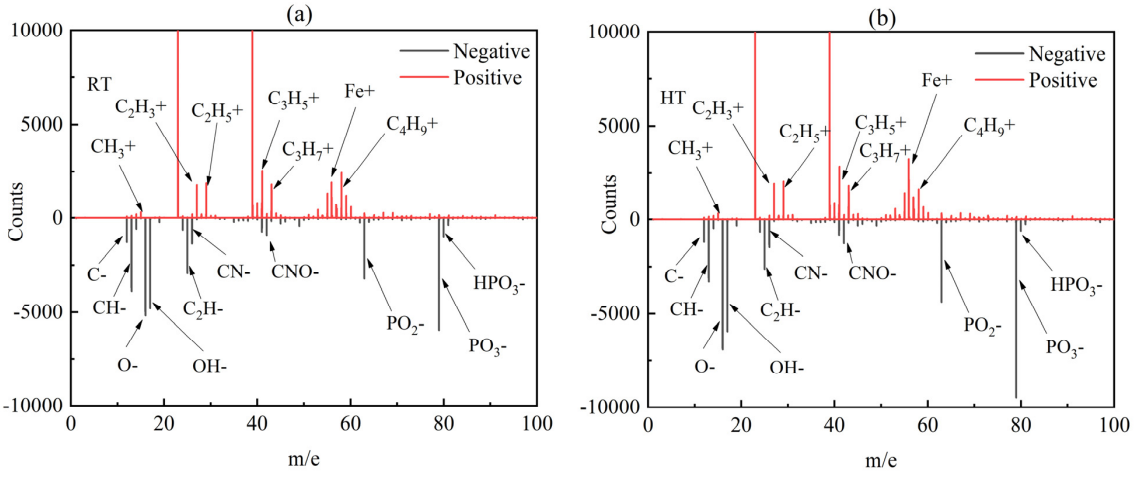

Figure 8. TOF-SIMS analysis of ions derived from the disc rub track oiled by 0.5 wt% IL-NPAS-0.5 additive at 25 °C (**a**) and under 100 °C (**b**) temperatures.

4. Conclusions

In this investigation, we synthesized a novel phosphate ammonium salt (IL-NPAS) as an eco-friendly, sulphur-free lubricant additive and compared its performance with that of a commercially available additive, amine salts of phosphoric acid esters (AW6110), at concentrations of 0.1 and 0.5 wt% in 150 SN base oil. At the lower concentration (0.1 wt%), neither additive significantly declined the coefficient of friction (COF); however, both markedly decreased wear volume by 65–70% compared with the neat oil across both temperatures. At the higher concentration (0.5 wt%), both additives exhibited stable COF values, showing a consistent reduction of 34–36% relative to the base oil, along with an 80–85% decrease in wear volume at 25 °C. Under high-temperature conditions (100 °C), the IL-NPAS additive demonstrated particularly high efficacy, reducing the COF by 40–45% and wear volume by 85–90% compared with the 150 SN basic lubricant. Overall, IL-NPAS and AW6110 additives presented comparable lubrication performance.

The morphological analysis by SEM revealed that adhesive wear dominated at low temperatures, whereas adhesive wear was accompanied by abrasive wear at 100 °C temperatures. The IL-NPAS and AW6110 additives exhibited similar wear patterns consistent with the tribological results. The XPS analysis confirmed the formation of a tribofilm via tribochemical reactions between the IL-NPAS addition and the steel substrate surface. The tribofilm consists of iron phosphate, FeO, Fe_2O_3, and FeOOH compounds. Furthermore, TOF-SIMS analysis provided additional evidence of these tribochemical reactions, revealing intense Fe^+ ion signals and hydrocarbon-derived $C_xH_y^+$ fragments, features consistent with the presence of inorganic oxides and phosphate-based salts in the tribofilm. Briefly, these results demonstrated that the IL-NPAS addition enhanced the wear resistance of steel–steel contacts, thereby improving the durability of tribological components.

In summary, the lubrication performance of the synthesized IL-NPAS was comparable to that of the commercial AW6110 additive, but the proposed halogen-free additive stands out for its environmental compatibility and its potential for low-cost manufacturing, particularly in emerging economies. Therefore, the IL-NPAS additive opens prospects for producing low-cost additives on a larger scale. For scaling the applicability of the IL-NPAS additive for industrial use in various tribosystems, future studies should investigate its performance in mitigating electrochemical corrosion when formulated with various base oils. Additionally, further tribological testing under a wider range of operating conditions is essential. Compatibility assessments with rubber materials (oil sealing) should also be conducted to achieve long-term reliability.

Author Contributions: Conceptualization, M.K.A.A.; Methodology, J.X., S.H., Z.G. and C.Z.; Validation, F.Z.; Formal analysis, S.H., C.L. and F.Z.; Investigation, J.X., C.L. and C.Z.; Resources, F.Z. and C.Z; Data curation, S.H., C.L. and Z.G.; Writing—original draft, J.X., C.Z. and M.K.A.A.; Writing—review & editing, M.K.A.A.; Visualization, C.L. and M.K.A.A.; Supervision, C.Z. and M.K.A.A.; Project administration, C.Z and M.K.A.A. All authors have read and agreed to the published version of the manuscript.

Funding: The following funding agencies: The National Key R&D Program of China (2022YFB4003300), National Natural Science Foundation of China (U21A2046, 52475226), Youth Innovation Promotion Association CAS (2022429), the Gansu Province Science and Technology Plan (Grants 23ZDGA011, 24JRRA043), Taishan Scholars Program (tsqn202312299), Natural Science Foundation of Shandong Province (ZR2022ZD09).

Data Availability Statement: The original contributions presented in the study are included in the article, further inquiries can be directed to the corresponding author.

Conflicts of Interest: Authors Junjie Xie, Cunqiang Liu, Ziqiang Gao and Faxue Zhang were employed by the company Gansu Road & Bridge Construction Group Co., Ltd. The remaining authors declare

that the research was conducted in the absence of any commercial or financial relationships that could be construed as a potential conflict of interest.

References

1. Luo, J.; Liu, M.; Ma, L. Origin of friction and the new frictionless technology—Superlubricity: Advancements and future outlook. *Nano Energy* **2021**, *86*, 106092. [CrossRef]
2. Humphrey, E.; Morris, N.; Leighton, M.; Rahmani, R.; Rahnejat, H. Multiscale friction in lubricant-surface systems for high-performance transmissions under mild wear. *Tribol. Lett.* **2018**, *66*, 77. [CrossRef]
3. Ali, M.K.A.; Xianjun, H.; Mai, L.; Qingping, C.; Turkson, R.F.; Bicheng, C. Improving the tribological characteristics of piston ring assembly in automotive engines using Al_2O_3 and TiO_2 nanomaterials as nano-lubricant additives. *Tribol. Int.* **2016**, *103*, 540–554. [CrossRef]
4. Zhou, Y.; Qu, J. Ionic liquids as lubricant additives: A review. *ACS Appl. Mater. Interfaces* **2017**, *9*, 3209–3222. [CrossRef] [PubMed]
5. Kontham, V.; Padmaja, K.V.; Madhu, D. Synthesis of ricinoleate anion based ionic liquids and their application as green lubricating oil additives. *J. Saudi Chem. Soc.* **2020**, *24*, 742–753. [CrossRef]
6. Yang, Z.; Guo, B.; Liang, Y.; Huang, Q.; Li, F.; Wang, R.; Yan, X.; Yu, B.; Yu, Q.; Cai, M. Performance of oil-soluble ionic liquids as novel lubricant additives. *J. Mol. Liq.* **2022**, *363*, 119837. [CrossRef]
7. Zhou, Q.; Lu, X.; Zhang, S.; Guo, L. Physicochemical properties of ionic liquids. In *Ionic Liquids Further UnCOILed*; Plechkova, N.V., Seddon, K.R., Eds.; Wiley: Hoboken, NJ, USA, 2014. [CrossRef]
8. Wang, M.; He, H.; Fang, X.; Li, H. The development status and future trends of lubricant additives technology: Based on patents analysis. *PLoS ONE* **2024**, *19*, e0304888. [CrossRef] [PubMed]
9. Patel, J.R.; Chauhan, K.V.; Rawal, S.; Patel, N.P.; Subhedar, D. Advances and challenges in bio-based lubricants for sustainable tribological applications: A comprehensive review of trends, additives, and performance evaluation. *Lubricants* **2025**, *13*, 440. [CrossRef]
10. Ali, M.K.A.; Liang, Y.; Sun, Y.; Zhang, C.; Yu, Q.; Hu, S.; Zhou, F.; Liu, W. Development of a high-performance lubricant based on halogen-free phosphonium ionic liquid for electrified vehicle transmissions. *Tribol. Int.* **2026**, *214*, 111206. [CrossRef]
11. Yang, K.; Xiong, Y.; Wu, G.; Lin, H.; Tang, J.; Wu, C.; Chen, H.; Wang, Y. Multi-dimensional nano-additives for their superlubricity: Tribological behaviors and lubrication mechanisms. *Adv. Mater. Interfaces* **2025**, *12*, 2400796. [CrossRef]
12. Adavodi, R.; Dini, G. Benzotriazoium bis (2-ethylhexyl) phosphate ionic liquid as a catalyst and multifunctional lubricant additive: Synthesis, optimization, characterization, and tribological evaluation. *Arab. J. Sci. Eng.* **2024**, *49*, 7995–8010. [CrossRef]
13. Jia, S.; Qin, J.; Chen, L.; Zhang, Y.; Mao, Y.; Lin, H.; Han, S. Tribological properties and synergistic lubrication mechanism between tetramethyl dodecyl diisooctyl phosphate ionic liquids and molybdenum-based metal organic frameworks additives. *Wear* **2025**, *576–577*, 206137. [CrossRef]
14. Ali, M.K.A.; Abdelkareem, M.A.A.; Elagouz, A.; Xianjun, H. In *Nanotechnology in the Automotive Industry*; Song, H., Nguyen, T.A., Yasin, G., Singh, N.B., Gupta, R.K., Eds.; Chapter 32—Nanolubricant additives. Elsevier: Amsterdam, The Netherlands, 2022; pp. 675–711.
15. Guan, B.; Pochopien, B.A.; Wright, D.S. The chemistry, mechanism and function of tricresyl phosphate (TCP) as an anti-wear lubricant additive. *Lubr. Sci.* **2016**, *28*, 257–265. [CrossRef]
16. Johnson, D.W. *The Tribology and Chemistry of Phosphorus-Containing Lubricant Additives*; IntechOpen: London, UK, 2016.
17. Xiong, L.; He, Z.; Xie, F.; Hu, J.; Liu, J.; Han, S.; Yang, S. Study of tribological synergistic effect of N-containing heterocyclic borate ester with tricresyl phosphate as rapeseed oil additive. *Tenside Surfactants Deterg.* **2020**, *57*, 175–184. [CrossRef]
18. Jiang, L.; Duan, F. Tribological Properties of Tricresyl Phosphate Blended in Base Oils between Iron-Based Surfaces. *Langmuir* **2025**, *41*, 29064–29075. [CrossRef]
19. Ali, M.K.A.; Zhang, C.; Sun, Y.; Yu, Q.; Zhou, Z.; Zhou, F.; Liu, W. Electro-controlled friction and tribofilm formation on electrified steel surfaces lubricated with an N/P-based ionic liquid additive under sliding conditions. *Wear* **2025**, 580–581, 206251. [CrossRef]
20. Cui, S.; Wan, S.; Zhu, Q.; Tieu, A.K.; Zhu, H.; Wang, L.; Cowie, B. Tribochemical behavior of phosphate compounds at an elevated temperature. *J. Phys. Chem. C* **2016**, *120*, 25742–25751. [CrossRef]
21. Li, Z.; Dolocan, A.; Morales-Collazo, O.; Sadowski, J.T.; Celio, H.; Chrostowski, R.; Brennecke, J.F.; Mangolini, F. Lubrication mechanism of phosphonium phosphate ionic liquid in nanoscale single-asperity sliding contacts. *Adv. Mater. Interfaces* **2020**, *7*, 2000426. [CrossRef]
22. Li, H.; Zhang, Y.; Li, C.; Zhou, Z.; Nie, X.; Chen, Y.; Cao, H.; Liu, B.; Zhang, N.; Said, Z. Extreme pressure and antiwear additives for lubricant: Academic insights and perspectives. *Int. J. Adv. Manuf. Technol.* **2022**, *120*, 1–27. [CrossRef]
23. Beeck, O.; Givens, J.; Williams, E. On the mechanism of boundary lubrication. II. Wear prevention by addition agents. *Proc. R. Soc. Lond. Ser. A Math. Phys. Sci.* **1940**, *177*, 103–118.
24. Forbes, E.; Battersby, J. Application of adsorption/reaction mechanism to load-carrying results. *ASLE Trans.* **1974**, *17*, 268–270.

25. Oshio, T. Anti-Wear Properties and Mechanisms of Dialkyl Phosphonates in Ester Base Oils. Ph.D. Thesis, Ecole Centrale de Lyon, Écully, France, 2023. Available online: https://bibliotheque.ec-lyon.fr/documents/TH_2023ECDL0029.pdf (accessed on 1 December 2025).
26. Johnson, D.W.; Hils, J.E. Phosphate Esters, Thiophosphate Esters and Metal Thiophosphates as Lubricant Additives. *Lubricants* **2013**, *1*, 132–148. [CrossRef]
27. Xue, Q.; Liu, W. Tribochemistry and the development of AW and EP oil additives—A review. *Lubr. Sci.* **1994**, *7*, 81–92. [CrossRef]
28. Naveira-Suarez, A.; Tomala, A.; Grahn, M.; Zaccheddu, M.; Pasaribu, R.; Larsson, R. The influence of base oil polarity and slide–roll ratio on additive-derived reaction layer formation. *Proc. Inst. Mech. Eng. Part J J. Eng. Tribol.* **2011**, *225*, 565–576. [CrossRef]
29. Zhao, G.; Wu, X.; Li, W.; Wang, X. Hydroquinone bis (diphenyl phosphate) as an antiwear/extreme pressure additive in polyalkylene glycol for steel/steel contacts at elevated temperature. *Ind. Eng. Chem. Res.* **2013**, *52*, 7419–7424. [CrossRef]
30. Minami, I.; Mori, S. Concept of molecular design towards additive technology for advanced lubricants. *Lubr. Sci.* **2007**, *19*, 127–149. [CrossRef]
31. Zhang, D.; Suo, X.; Wang, J.; Wang, Y.; Fan, F.; Wang, L. The synergistic effect of novel anti-wear additive 1,3,4-thiadiazole mixed ammonium salt and MoDTC on tribological properties of FeCoCrNiMn alloy. *J. Mater. Res. Technol.* **2025**, *38*, 5235–5249. [CrossRef]
32. Cai, M.; Yu, Q.; Liu, W.; Zhou, F. Ionic liquid lubricants: When chemistry meets tribology. *Chem. Soc. Rev.* **2020**, *49*, 7753–7818. [CrossRef]
33. Adhvaryu, A.; Erhan, S.; Perez, J. Tribological studies of thermally and chemically modified vegetable oils for use as environmentally friendly lubricants. *Wear* **2004**, *257*, 359–367. [CrossRef]
34. Ali, M.K.A.; Sun, Y.; Zhang, C.; Yu, Q.; Zhao, C.; Zhou, F.; Liu, W. Improving tribological performance of electrified steel interfaces in e-mobility systems using ash-sulfur-less oil additives based on amine salts-phosphoric esters. *Tribol. Int.* **2025**, *205*, 110561. [CrossRef]
35. King Industries, I. Product Data Sheet for Amine Salts of Aliphatic Phosphoric Acid Esters (NA-LUBE® AW-6110). 2023. Available online: https://www.kingindustries.com/assets/1/6/NA-LUBE_AW-6110_PDS.pdf?1126 (accessed on 1 December 2025).
36. Itoh, T. Ionic liquids as tool to improve enzymatic organic synthesis. *Chem. Rev.* **2017**, *117*, 10567–10607. [CrossRef] [PubMed]
37. Ma, R.; Li, W.; Zhao, Q.; Zheng, D.; Wang, X. In situ synthesized phosphate-based ionic liquids as high-performance lubricant additives. *Tribol. Lett.* **2019**, *67*, 60. [CrossRef]
38. Phillips, W.D.; Milne, N. Ashless phosphorus–containing lubricating oil additives. In *Lubricant Additives*; CRC Press: Boca Raton, FL, USA, 2017; pp. 157–196.
39. Truhan, J.J.; Qu, J.; Blau, P.J. A rig test to measure friction and wear of heavy duty diesel engine piston rings and cylinder liners using realistic lubricants. *Tribol. Int.* **2005**, *38*, 211–218. [CrossRef]
40. Barnhill, W.C.; Luo, H.; Meyer, H.M., III; Ma, C.; Chi, M.; Papke, B.L.; Qu, J. Tertiary and quaternary ammonium-phosphate ionic liquids as lubricant additives. *Tribol. Lett.* **2016**, *63*, 22. [CrossRef]
41. Zhang, M.; Liu, H.; Zhang, E.; Chen, Y.; Li, W.; Cheng, S. Tribological performance of fatty acid ammonium ionic liquids as anti-wear additives in water-based fluids. *Tribol. Int.* **2024**, *194*, 109565. [CrossRef]
42. Yan, J. Design of Ionic Liquid Based Additives for Integration with Modern Lubrication Systems. Ph.D. Thesis, The University of Texas at Austin, Austin, TX, USA, 2025.
43. Somers, A.E.; Yunis, R.; Armand, M.B.; Pringle, J.M.; MacFarlane, D.R.; Forsyth, M. Towards phosphorus free ionic liquid anti-wear lubricant additives. *Lubricants* **2016**, *4*, 22. [CrossRef]
44. Xiang, W.; Zhao, C.; Zhang, C.; Wang, X.; Li, X.; Liu, S.; Sun, C.; Yu, Q.; Yu, B.; Cai, M.; et al. Halogen-free functional quaternary ammonium-based ionic liquid as an ecofriendly corrosion inhibitor for Q235 steel in acids. *Langmuir* **2024**, *40*, 389–402. [CrossRef]
45. Bansal, V.; Sastry, M.; Sarpal, A.; Jain, S. Characterization of nitrogen and phosphorous componenets in a multifunctional lubricant additive by NMR and IR techniques. *Tribol. Lubr. Technol.* **1997**, *53*, 17.
46. Ewen, J.P.; Latorre, C.A.; Gattinoni, C.; Khajeh, A.; Moore, J.D.; Remias, J.E.; Martini, A.; Dini, D. Substituent effects on the thermal decomposition of phosphate esters on ferrous surfaces. *J. Phys. Chem. C* **2020**, *124*, 9852–9865. [CrossRef]
47. Qu, G.; Fang, H.; Li, Y.; Zhang, S.; Hu, L. Combining in-situ quadrupole mass spectrometer analyses: Study on the structure–activity relationship and lubrication mechanisms of ammonium phosphate ionic liquids. *J. Mol. Liq.* **2024**, *413*, 125998. [CrossRef]
48. Fan, M.; Song, Z.; Liang, Y.; Zhou, F.; Liu, W. Laxative inspired ionic liquid lubricants with good detergency and no corrosion. *ACS Appl. Mater. Interfaces* **2014**, *6*, 3233–3241. [CrossRef]
49. Wang, X.; Jin, L.; Zhang, H.; Xu, R.; Stelmakh, O.; Jin, Z.; Liu, Y. Wear mechanism of steel materials oxide form conversion at the friction interface conducted by lubricants containing varying hydrogen. *Friction* **2025**, *13*, 9440934. [CrossRef]
50. Li, S.; Wang, X.; Jiang, S.; Han, S.; Wang, C. Tribological mechanisms of the synergistic effect between phosphate based ionic liquids and metal-organic frameworks. *Wear* **2024**, *558*, 205565. [CrossRef]

51. Huang, G.; Sun, L.; Li, L.; Pei, L.; Xue, W.; Wang, R.; Wang, Y. Exploring the effect mechanism of alkyl chain lengths on the tribological performance of ionic liquids. *ACS Omega* **2024**, *9*, 3184–3192. [CrossRef]
52. Zhang, C.; Wang, X.; Sun, Y.; Sun, S.; Zhao, C.; Liu, Y.; Yang, S.; Yu, Q.; Ali, M.K.A. Synthesis of a Novel Multifunctional Ionic Liquid Based on Benzotriazole for Enhanced Tribological Performance of Steel Interfaces. *Tribol. Lett.* **2025**, *73*, 64. [CrossRef]
53. Xu, Z.; Li, S.; Guo, C.; Li, Z.; Liang, H. Change of surface oxide layer of pyrite samples prepared by resin embedding polishing method after long-term placement and its effect on TOF-SIMS analysis. *Surf. Interfaces* **2024**, *46*, 104124. [CrossRef]